

Novel β -Distonic Radical Cations $[C_nH_{2n+2}S]^+$ ($n = 2, 3$) Formed upon Decarbonylation of Ionized *S*-Alkyl Thioformates: A Mass Spectrometric and *ab Initio* Study

Robert Flammang,^{*,†} Driss Lahem,[†] and Minh Tho Nguyen^{*,‡}

Laboratory of Organic Chemistry, University of Mons-Hainaut, Avenue Maistriau 19, B-7000 Mons, Belgium, and Department of Chemistry, University of Leuven, Celestijnenlaan 200F, B-3001 Leuven, Belgium

Received: June 10, 1997; In Final Form: October 13, 1997[⊙]

Decarbonylation is commonly observed in the 70 eV electron impact mass spectra of a series of *S*-alkyl thioformates, $H-C(=O)SR$ **1–7**. Using a combination of collisional activation (CA) and neutralization–reionization (NR) mass spectra, it is shown that the spectra of the so-formed $[M-CO]^+$ ions differ from the isomeric alkane thiol ions (RSH^+), if $R > CH_3$. These fragment ions are therefore distonic radical cations, and given the fact that the α -distonic $\cdot CH_2-S^+H_2$ ions are not present under our experimental conditions, it is proposed that they actually are β -distonic ions. Strong evidence for the distonic nature of the fragment ions derived from **2–7**⁺ has been obtained owing to the use of a new hybrid tandem mass spectrometer presenting a sector–quadrupole–sector configuration. In the case of ethyl derivatives ($R = C_2H_5$), both the distonic $\cdot CH_2CH_2S^+H_2$ (**2b**) and conventional $CH_3CH_2SH^+$ (**2a**) ions are observed. The nonclassical structure **2b** reacts indeed with nitric oxide ($NO\cdot$) giving the production of H_2S^+-NO ions (m/z 64), characterized by high-energy collisional activation. Distonic ions **2b** have also been otherwise prepared in an ion–molecule reaction involving the transfer of ionized ethene from $\cdot CH_2CH_2O^+=CH_2$ to neutral hydrogen sulfide, H_2S . Upon CA, the resulting ions **2b** show the same behavior as the product of decarbonylation of the *S*-ethyl thioformate molecular ions. Upon neutralization–reionization, the distonic isomers of the alkane thiol ions give rise to intense peaks corresponding to H_2S^+ and ionized olefins. Portions of the potential energy surface related to the rearrangement and dissociation processes in the $[C_2H_6S]^+$ system have also been constructed using *ab initio* molecular orbital calculations at the QCISD(T)/6-311++G(d,p)//UMP2/6-31G(d,p) level. Theoretical results provide further support for the observation of β -distonic ions.

Introduction

Distonic radical cations are species in which both charge and radical sites are formally separated.¹ Their properties have been explored in the gas phase by a variety of mass spectral methods.^{2,3} In particular, the β -distonic isomer of the ethanol radical cation has been studied extensively. This $\cdot CH_2CH_2OH_2^+$ ion was calculated^{4,5} to be about 42 kJ/mol lower in energy than the classical radical cation of ethanol and to have a substantial binding energy with respect to dissociation into $C_2H_4^+$ and H_2O (about 83 kJ/mol). These theoretical predictions^{4,5} sparked a wide interest in the unusual isomer of ionized ethanol. Using collisional activation (CA) mass spectrometry, Terlouw et al.⁶ have demonstrated that the fragment ion $C_2H_6O^+$ of 1,3-propanediol has a distinct structure from the well-characterized ethanol or dimethyl ether radical cations. The reactivity of the β -distonic ion toward a few neutral reagents was also found to be different from that of its conventional isomer, ionized ethanol.⁷ In sharp contrast, only limited information is now available on the analogous $C_2H_6S^+$ system. Previous calculations on the latter have made use of a low-level of theory⁸ to study a 1,2-SH₂ migration in the ethene-sulfonium radical cation, $\cdot CH_2CH_2SH_2^+$. Only a brief experimental description³ of this distonic ion has been reported: it was assumed that it could be generated by an ion–molecule reaction, involving an ethene ion transfer, between the distonic ion $\cdot CH_2CH_2O^+=CH_2$ with neutral H_2S .

In the course of an extensive study of the unimolecular chemistry of a series of *S*-alkyl thioformate, $H-C(=O)SR^+$,

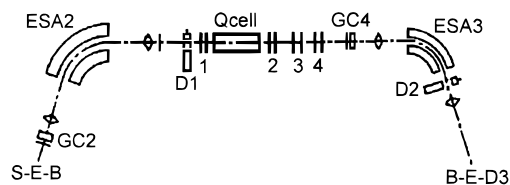


Figure 1. Schematic representation of the intermediate region of the Micromass AutoSpec 6F mass spectrometer (hybrid configuration): GC, gas cell; D, off-axis photomultiplier detector; 1, deceleration lens; 2, reacceleration lens; 3, Y/Z lenses; 4, demagnification lens.

radical cations,^{9,10} we have observed that decarbonylation of the molecular ions was a common process. We have therefore investigated the $[C_nH_{2n+2}S]^+$ ions making use of tandem mass spectrometry methodologies such as collisional activation (CA) and neutralization–reionization (NR) mass spectrometries. In its hybrid configuration, the tandem mass spectrometer has also allowed the study of some ion–molecule reactions to be carried out. To obtain additional quantitative information, *ab initio* MO calculations at the QCISD(T)/6-311++G(d,p)//UMP2/6-31G(d,p) level of theory have also been carried out to characterize the product of decarbonylation of ionized *S*-ethyl thioformate, the $[C_2H_6S]^+$ ions.

Experimental Section

The spectra have been recorded on a large-scale tandem mass spectrometer of EBEEBE geometry (E stands for electric sector and B for magnetic sector) fitted with five collision cells and, in the hybrid configuration, with an additional rf-only quadrupole collision cell. Some characteristics of the spectrometer, schematically presented in Figure 1, have already been presented in previous papers.^{11–13} General conditions of the experiments

[†] University of Mons-Hainaut.

[‡] University of Leuven.

[⊙] Abstract published in *Advance ACS Abstracts*, December 1, 1997.

were 8 kV accelerating voltage, 200 μ A trap current, 70 eV ionizing electron energy, and 200 °C ion source temperature. The liquid samples were introduced in the source via a heated (180 °C) septum inlet.

Unless otherwise stated, CA and NR spectra were recorded by scanning the field of the third electric sector and collecting the ions in the fifth field-free region with an off-axis photomultiplier detector. In the hybrid arrangement, a demagnification lens actually replaces the neutralization cell.

The ion–molecule reactions were performed in the quadrupole collision cell floated at ca. 7995 V. The ions produced in the quadrupole, reaccelerated at 8 keV, were separated by scanning the field of the second magnet while the CA (N_2) spectra of mass-selected products were recorded by a conventional scanning of the field of the last electric sector.

The alkane thiols were commercially available (Aldrich), while the *S*-alkyl thioformates **1–7** were prepared according to literature methods.¹⁴

Results and Discussion

1. Molecular Orbital Calculations of the $[C_2H_6S]^{\bullet+}$ Potential Energy Surface. To obtain some quantitative data on the unimolecular rearrangements and fragmentations of the $[C_2H_6S]^{\bullet+}$ ions that could be helpful for the understanding of the experimental observations, we have carried out quantum chemical calculations on the relevant portions of the potential energy surface. To facilitate the discussion, the theoretical results will be first reported in this section.

Ab initio molecular orbital calculations were performed with the aid of the Gaussian 94 set of programs.¹⁵ The stationary points were initially located at the unrestricted Hartree–Fock level (UHF) in conjunction with the polarized 6-31G(d,p) basis set and characterized by harmonic vibrational frequencies at this level. Geometrical parameters of the relevant equilibrium and transition structures were then reoptimized at the second-order perturbation theory level ((U)MP2/6-31G(d,p)). The potential energy curves were subsequently mapped out using electronic energies computed using the quadratic configuration interaction method with a larger basis set, QCISD(T)/6-311++G(d,p), based on (U)MP2/6-31G(d,p) optimized geometries and corrected for zero-point energies (ZPE). For the open-shell structures considered, the spin-contamination in UHF reference wave functions lies within an acceptable range for equilibrium structures and somewhat larger for transition structures, but the $\langle S^2 \rangle$ values for transition structures are however smaller than 0.9. As a consequence, some barrier heights may be overestimated. Because the energetic results obtained from the present computations are rather moderately accurate, we put more importance on the qualitative aspect of the energy surface, which helps the experimental findings to be understood, rather than on the absolute values. While Table 1 lists the total and relative energies of all the structures considered, Figure 2 displays only the selected geometrical parameters of three $[C_2H_6S]^{\bullet+}$ isomers, **2a**, **2b**, and **2c**, and the transition structure (TS) having the lowest energy among the TSs. Figure 3 illustrates a schematic potential energy profile showing the interconnections and dissociations of the ion isomers. Figure 3 and Table 1 also include the energies of the fragments $CH_3CH=SH^+ + H^{\bullet}$ (**2d**), $CH_2=CH-SH_2^+ + H^{\bullet}$ (**2e**), and $H_2C=CH_2 + SH_2^{\bullet+}$ (**2f**). In general, **x/y** stands for a TS connecting both equilibrium structures **x** and **y**.

Figure 3 shows that the ionized ethane thiol $CH_3CH_2SH^{\bullet+}$ is the most stable isomer lying about 55 and 64 kJ/mol below both the β -distonic $CH_2CH_2SH_2^{\bullet+}$ (**2b**) and α -distonic $CH_3CHSH_2^{\bullet+}$ (**2c**) species, respectively. This is in clear contrast

TABLE 1: Total (Hartree) and Relative (kJ/mol) Energies of the $[C_2H_6S]^{\bullet+}$ Structures Considered at the QCISD(T)/6-311++G(d,p) Level of MO Theory

structure	total energy ^a	ZPE ^b	relative energy ^c
$CH_3CH_2SH^{\bullet+}$ (2a)	-476.968 02	187	0
$CH_2CH_2SH_2^{\bullet+}$ (2b)	-476.943 67	178	55
$CH_3CHSH_2^{\bullet+}$ (2c)	-476.940 50	178	64
$CH_3CHSH^+ + H^{\bullet}$ (2d)	-476.897 32	160	158
$CH_2=CH-SH_2^+ + H^{\bullet}$ (2e)	-476.875 44	158	214
$CH_2=CH_2 + SH_2^{\bullet+}$ (2f)	-476.894 06	166	174
TS 2a/2b	-476.914 38	173	127
TS 2a/2c	-476.904 65	172	152
TS 2b/2c	-476.871 63	168	235
TS 2a/2d	-476.893 02	165	175
TS 2b/2e	-476.863 00	158	247
TS 2c/2d	-476.892 91	163	174
TS 2c/2e	-476.869 05	159	232

^a Based on (U)MP2/6-31G(d,p) optimized geometries. ^b Zero-point energies based on (U)HF/6-31G(d,p) harmonic vibrational wavenumbers and scaled by 0.9. ^c Relative energies including QCISD(T)/6-311++G(d,p) values and ZPE corrections.

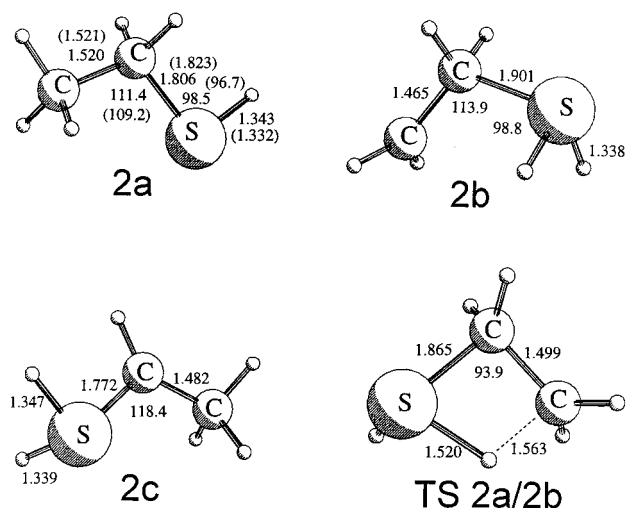


Figure 2. Selected geometrical parameters at the UMP2/6-31G(d,p) level of ethane thiol ion $CH_3CH_2SH^{\bullet+}$ (**2a**) (parameters of the neutral form in parentheses) and two distonic isomers **2b** and **2c** and the transition structure for 1,3-H shift connecting **2a** and **2b**. Bond lengths are given in angstroms and bond angles in degrees.

with the situation in oxygen analogs $C_2H_6O^{\bullet+}$ mentioned above, but in line with the energy ordering in the lower homologous $[CH_4S]^{\bullet+}$ system, where the methane thiol ion $CH_3SH^{\bullet+}$ is more stable than the α -distonic $CH_2SH_2^{\bullet+}$.¹⁶

The most interesting result given in Figure 3 is perhaps the fact that both isomers **2a** and **2b** are connected to each other by a direct 1,3-shift of the hydrogen via the TS **2a/2b** rather than by two consecutive 1,2-shifts. In particular, isomerization between both distonic species **2b** and **2c** is prohibited by a substantial energy barrier, namely 180 kJ/mol relative to **2b**. It has been established that the 1,3-H shift is a difficult process in the neutral state but becomes strongly accelerated upon ionization.¹⁷ In addition, the low-energy position of TS **2a/2b**, which lies well below both dissociation limits $CH_3CH=SH^+ + H^{\bullet}$ (**2d**) and $H_2C=CH_2 + SH_2^{\bullet+}$ (**2f**), suggests that the ion system is likely to undergo a preliminary isomerization **2a** \rightarrow **2b** before dissociating into fragments. Within the expected accuracies of our calculations, on relative energies, it can only be stated that both the H loss from the central carbon of **2a**^{•+} and the elimination of $SH_2^{\bullet+}$ from **2b**^{•+} are competitive processes.

Of the two $(C_2H_5S)^{\bullet+}$ ion fragments, the cation $CH_3CH=SH^+$ (in **2d**) is unambiguously more stable (by 56 kJ/mol) than its

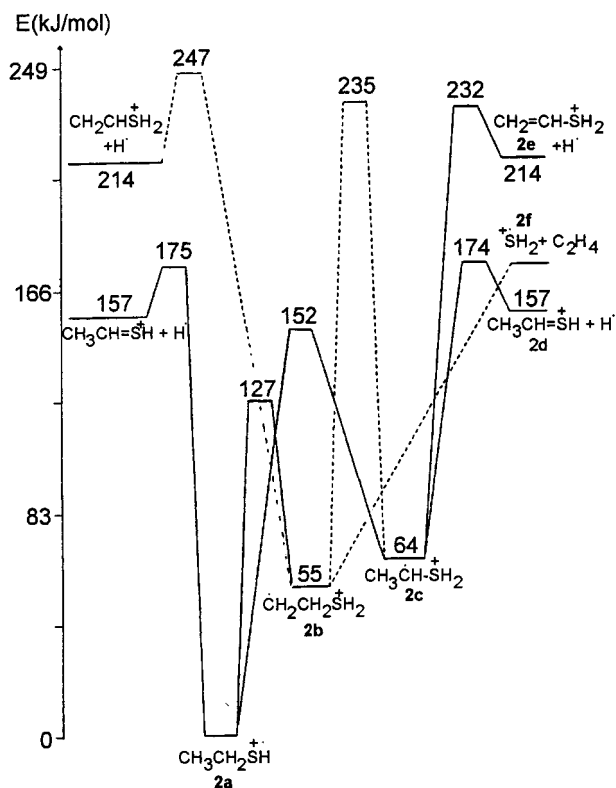


Figure 3. Schematic potential energy profiles showing the isomerizations and fragmentations of the $[C_2H_6S]^+$ ion isomers. Relative energies are obtained from QCISD(T)/6-311++G(d,p)//UMP2/6-31G(d,p)+ZPE calculations.

TABLE 2: Relative Abundance (%) of $[M-CO]^+$ Ions in the EI Mass Spectra (70 eV) of Thioformates $HC(=O)SR$, 1–7

ions	R =	thioformate						
		1	2	3	4	5	6	7
M^+	Me	100	100	33	25	9	5	4
$[M-CO]^+$	Et	26	31	12	32	9	5	3
	iPr							
	nPr							
	nBu							
	iBu							
	sBu							

$CH_2=CHSH_2^+$ isomer (in **2e**). The former is in fact the protonated form of both thioacetaldehyde $[CH_3C(=S)H]$ and mercaptan $[CH_2=CHSH]$ isomers.

2. Decarbonylation of *S*-Alkyl Thioformate Molecular Ions Studied by Mass Spectrometry. The unimolecular chemistry of the molecular ions of *S*-alkyl thioformates, $HC(=O)SR$ **1–7** (R = alkyl), has been shown to involve complex rearrangements supplemented by the competitive losses of HS^+ and H_2O .^{9,10} A loss of carbon monoxide is also detected for all the thioformates (Table 2), but the relative intensity of the corresponding peak decreases rapidly for the higher homologues. The description of experimental data will therefore be restricted here to the thioformates **1–4**. The reference ions used in the following are formed by direct ionization of the alkane thiols referred to as **1a–4a**.

The CA spectra of methane thiol radical cations **1a** and its distonic isomer $\cdot CH_2S^+H_2$ (**1b**), which can be generated by dissociative ionization of HSC_2H_4OH , have already been reported¹⁸ and found to be very similar to each other. The major difference was in fact seen in the intensity of the charge-stripping peak, which is more intense in the case of the distonic species. This spectral similarity has been ascribed to the fact that the barrier for interconversion lies below the dissociation threshold.¹⁶ We have reproduced these data and found moreover that the CA spectrum of the $[M-CO]^+$ ions of *S*-methyl

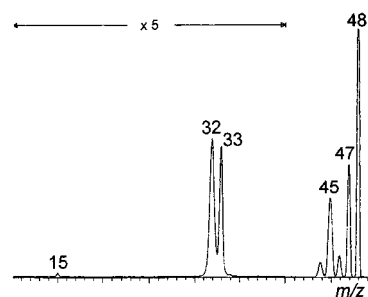


Figure 4. NR mass spectrum (NH_3/O_2) of the molecular ions of methane thiol **1a**.

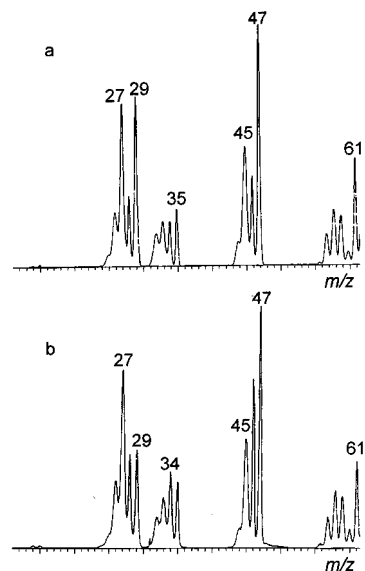
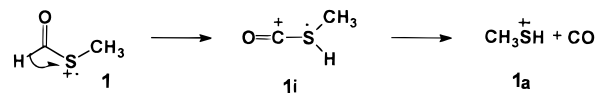


Figure 5. CA (N_2) spectrum of molecular ions of ethane thiol **2a** (m/z 62) (a) and CA (N_2) spectrum of the $[M-CO]^+$ ions of *S*-ethyl thioformate (**2**) (b).

SCHEME 1:



thioformate **1** is closer to the spectrum of the classical ions than to that of their distonic isomers.

As neutralization–reionization mass spectrometry has proved in numerous instances to be more structure-specific than the CA technique,¹⁹ we have also recorded the NR spectra. It turns out that the NR spectra of both isomeric ions are even more similar to each other than the corresponding CA spectra; a typical NR spectrum is shown in Figure 4. This is mainly due to the disappearance of the charge-stripping (CS) peak in the NR spectra, which is usually explained by a lower probability for the $m \rightarrow m^{2+}$ vertical ionization as compared to the $m^+ \rightarrow m^{2+}$ ionization.²⁰ In the present case, this can however be readily explained if the neutralized species do not survive in the NR experiment (vide infra). The proposed mechanism shown in Scheme 1 consists of a 1,2-hydrogen shift giving rise to the formation of a sulfurane intermediate ion **1i**. The occurrence of a hydrogen-bridged species cannot be ruled out, as they have been shown to play a crucial role in the decarbonylation of methyl formate.²¹

The $[M-28]^+$ ion of *S*-ethyl thioformate **2** is a mixture of isobars in similar abundances corresponding to the losses of both CO and C_2H_4 .²² The mass resolution of MS1 must therefore be increased in order to remove any interference. The CA spectra of the resulting $[M-CO]^+$ ions of **2** and the molecular spectra of alkane thiol **2a** are compared in Figure 5.

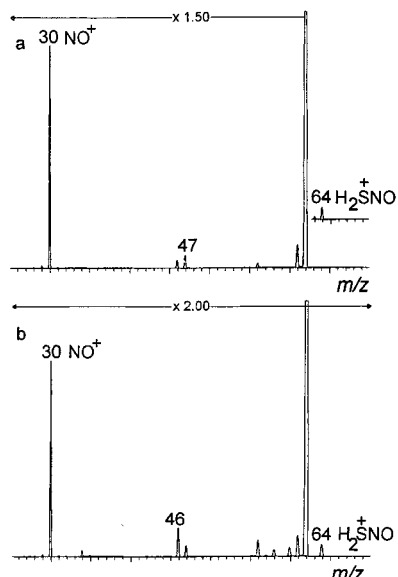


Figure 6. Reactions between ionized ethane thiol and NO^{\bullet} (a) and between $[M-CO]^{\bullet+}$ ions of *S*-ethyl thioformate and NO^{\bullet} (b) in an rf-only quadrupole collision cell.

Although these spectra are not very different, a closer comparison to the conventional ions generated from thiol **2a** points out that the fragment ions of $2^{+\bullet}$ present significant distinctions: (i) an increased intensity of the peaks at m/z 46, (ii) a decreased intensity of the peak at m/z 29 ($C_2H_5^+$), and (iii) the presence of a narrow peak at m/z 31 ascribed to charge stripping (CS). All these spectral variations point toward the production of an isomeric structure from ethane thiol radical cation **2a** and/or the presence of a mixture of structures in the decarbonylation process of $2^{+\bullet}$ ions. The rather facile interconversion between **2a** and its β -distonic isomer **2b** as revealed by MO calculations (see Figure 3) provides support for this interpretation.

Further evidence comes from the study of ion-molecule reactions within the rf-only quadrupole collision cell pressurized with nitric oxide. Weiske et al. have shown that the reaction of mass-isolated $\bullet CH_2-X-CH_3$ distonic ions ($X = Cl, Br$) and NO^{\bullet} generates exclusively CH_2NO^+ cations,²³ whereas their conventional $CH_3CH_2X^+$ isomers react only by electron transfer, giving NO^+ . Recent results in our laboratory have also shown that pyridine *N*-thioxide radical cations react very efficiently with NO^{\bullet} , producing ONS^+ .²⁴ NO^{\bullet} appears thus to be an excellent reagent for the differentiation of nonconventional and conventional isomeric ions. The spectra shown in Figure 6 correspond to the products observed when ethane thiol ions **2a** and $[2^{+\bullet}-CO]$ ions, decelerated down to ca. 5 eV, interact with NO^{\bullet} . In both spectra, not only a peak corresponding to charge exchange (m/z 30) is observed but also an interesting peak at m/z 64, which is more significant in the case of the reaction of the $[2^{+\bullet}-CO]$ ions. In the case of the reaction with **2a** ions, m/z 64 is present but constitutes less than 0.02% relative to the m/z 30. While the peak at m/z 46 corresponds to the product of unimolecular dissociation, the other peaks must arise from collision-induced dissociation even at the low kinetic energy used in the quadrupole. The CA spectrum of ions at m/z 64 (Figure 7) is dominated by peaks at m/z 30 (NO^+) and m/z 34 (H_2S^+); that means that the m/z 64 ions have the H_2S-NO^+ structure. Therefore, the charge exchange which is expected for the classical ions and the H_2S^+ transfer to NO^{\bullet} (giving H_2S-NO^+ ions) corroborate further our conclusions stated above concerning the production of a mixture of isomers containing both conventional ions **2a** and distonic species $\bullet CH_2CH_2S^+H_2$ (**2b**) during the decarbonylation of the $2^{+\bullet}$ molecular ions.

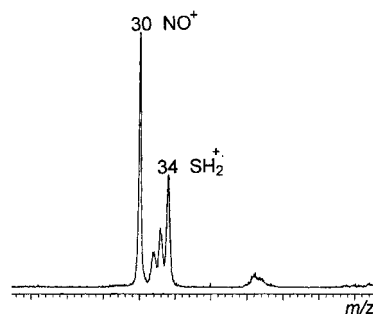
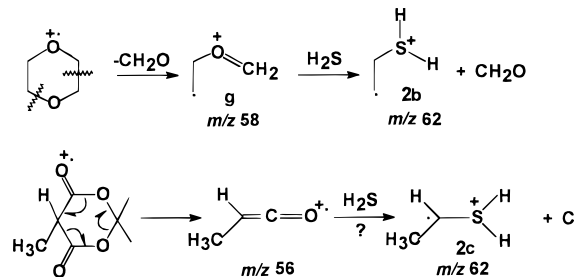


Figure 7. CA (N_2) spectrum of the m/z 64 ions generated by ion-molecule reaction between $[M-CO]^{\bullet+}$ ions of *S*-ethyl thioformate and NO^{\bullet} in an rf-only quadrupole collision cell.

SCHEME 2:



To obtain more data on the actual structure of the so-produced distonic ions, we have attempted to generate the $\bullet CH_2CH_2S^+H_2$ (**2b**) and $CH_3C^+HS^+H_2$ (**2c**) ions by using appropriate ion-molecule reactions (Scheme 2).

Dissociative ionization of 1,4-dioxane has been shown to produce in high yield the distonic ion **g**, $\bullet CH_2CH_2O^+=CH_2$.²⁵ It is now well-established²⁶ that this ion is thermodynamically stable and does not interconvert with the isomeric cyclic form (ionized oxetane being estimated to be 21 kJ mol⁻¹ less stable than the distonic structure **g**).²⁷ Moreover, gas-phase reactions of distonic ion **g** were investigated with different neutral reagents since this ion is a potentially useful tool for the synthesis of gaseous β -distonic ions.^{28,29} The most interesting bimolecular reactions revealed by these studies are dissociative electron transfer and transfer of ionized ethene to most of the neutral reagents. However, in all those cases where charge exchange is not thermodynamically favored (that means, ionization energy of the neutral reagent >9.2 eV), transfer of ionized ethene to the neutral reagent takes place. In the present work, ions **g** are prepared in the EI ion source, accelerated at 8 kV, mass-selected using a combination of the first three sectors (EBE), and focalized into the rf-only quadrupole collision cell. This cell was floated at ca. 7995 V and pressurized with H_2S (IE = 10.45 eV) at an estimated pressure of 10⁻³ Torr. The CA spectrum of so-formed m/z 62 ions turns out to be similar to that derived from $[M-CO]^{\bullet+}$ ions of **2**. This confirms on the one hand that the distonic ions which participate in the mixture are the β -distonic ions **2b** and on the other hand that the occurrence of the more stable conventional **2a** ions is due to postcollisional isomerization.

Neutral ketene³⁰ and methylketene³¹ were reported to transfer CH_2 or CH_3CH groups, respectively, to molecular ions of ketene, methylketene, and acetone. Also, ketene ions, CH_2CO^+ , were found to react with neutral reagents, ammonia for instance,³² resulting in a CH_2^+ transfer. Therefore, we have also attempted to employ ketene in related ion-molecule reactions.

Meldrum's acids are recognized to be excellent precursors of ketenes not only upon flash-vacuum pyrolysis conditions³³ but also upon dissociative ionization.³⁴ 2,2,5-Trimethyl-1,3-dioxane-4,6-dione was therefore ionized by electron impact, and

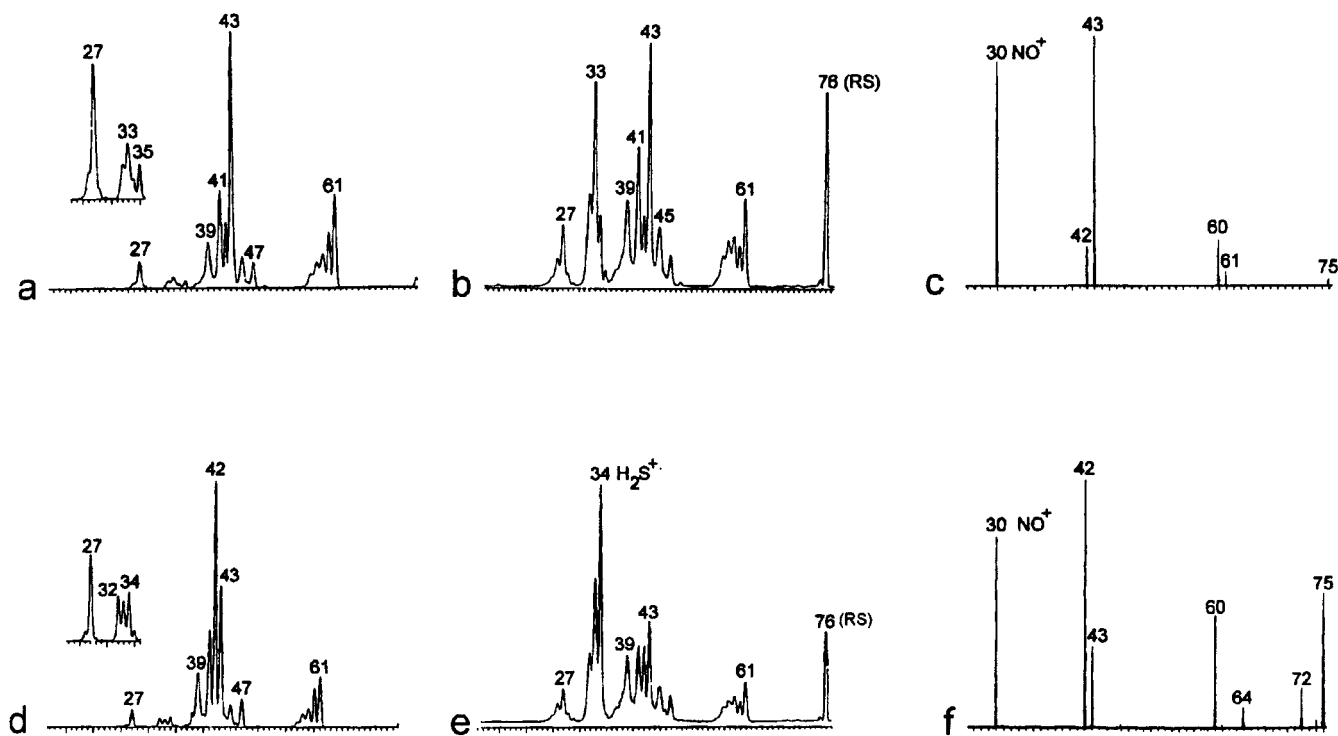
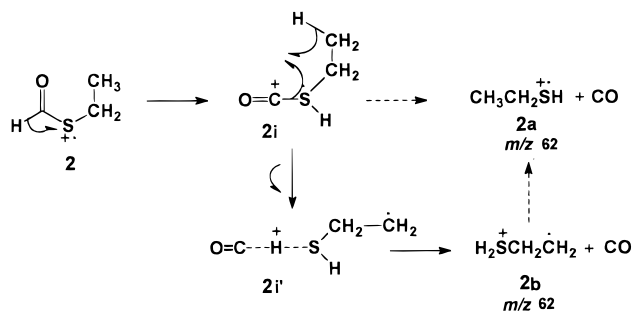


Figure 8. Comparison of the CA (O_2) spectra, NR (NH_3/O_2) spectra, and products of ion–molecule reaction with nitric oxide of the molecular ions of 2-propane thiol (a,b,c) and $[\text{M}-\text{CO}]^+$ ions of *S*-isopropyl thioformate (**4**) (d,e,f).

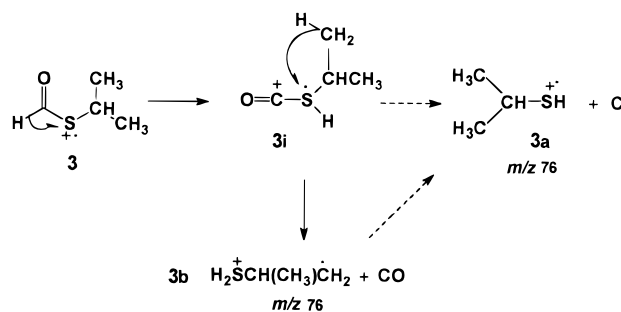
SCHEME 3:



the resulting m/z 56 ions were transferred in the quadrupole collision cell containing H_2S . Surprisingly, m/z 62 ions are actually formed under these conditions but with an extremely poor yield, so that interpretation of the CA data (similar to the data of ions **2b**) is not straightforward.

Taking all theoretical and experimental data together, we would suggest the reaction mechanism depicted in Scheme 3 for the decarbonylation of *S*-ethyl thioformate molecular ions. Briefly, this mechanism proposes the intermediacy of a sulfurane ion **2i**; simple cleavage of the S–CO bond should yield the classical ions **2a**. A hydrogen-bridged complex where a neutral and a radical are connected by a proton (Scheme 3) is supposed to be involved in the competing reaction pathway which yields the isomeric ions **2b**. This kind of complex has already been well described in the literature.³⁵ In fact, metastable peak shape analysis seems to contradict this proposal as the kinetic energy release ($T^{50} = 83$ meV) is quite high. However, the T^{22}/T^5 ratio (1.9₅) is slightly smaller than the ratio expected for a pure single-Gaussian profile (2.16).³⁶ The occurrence of a composite metastable peak shape is therefore not excluded. The sequence of hydrogen transfer may also start with the migration of a hydrogen of the methyl group, but that possibility appears unlikely as the first intermediate should be a destabilized sulfonium ion, $\text{HC}(\text{=O})\text{S}^+(\text{H})\text{CH}_2\text{CH}_2^*$. Further quantum chemi-

SCHEME 4:



cal calculations on decompositions of ionized methyl and ethyl thioformates are highly desirable to clarify this mechanistic point.

The experimental data related to *S*-isopropyl thioformate **3** ($[\text{M}-\text{CO}]^+$ ions) and 2-propane thiol molecular ions **3a** are collected in Figure 8. Differences in the CA spectra are even more clearly seen than in the previous cases. Accordingly, the base peak at m/z 43 for the classical ions (loss of SH^*) is replaced by a m/z 42 peak for the product of decarbonylation (loss of H_2S). Also, some significant differences appear in the low-mass region, in particular the increased intensity of the peak at m/z 34 corresponding to H_2S^+ . It is thus clear that isomers of 2-propane thiol ions **3a** are produced in the decarbonylation process, and the significant peaks at m/z 42 and 34 can be assigned to a distonic species **3b** (Scheme 4). However, the consistency of the abundance ratio of the m/z 61, 43, 41, and 39 peaks indicates that classical ions **3a** are expected to be present in appreciable quantity.

The CA results are fully confirmed by the NR experiments. In going from the classical ions to the decarbonylation products, a decreased intensity of the recovery signal and the peaks at m/z 61, 43, 41, and 39 can be detected; the same holds for m/z 33, which corresponds to the reionization of the neutral lost in the m/z 76 \rightarrow m/z 43 reaction. Reversely, peaks at m/z 34 and 42 are enhanced and correspond to H_2S^+ and propene,

respectively. It is therefore clear that the neutralization of the distonic species yields hypervalent diradicals which, at least in part,³⁷ are readily fragmented before reionization.

Additional evidence for the formation of distinct isomers is again provided by the study of ion–molecule reactions with nitric oxide. The spectrum shown in Figure 8c corresponds to the products observed when 2-propane thiol ions, slowed down to ca. 5 eV, interact with NO \bullet . The peak at m/z 30 corresponds to charge exchange, a reaction expected for classical ions if allowed by the ionization energies (very close indeed in the present case: IE(NO \bullet) = 9.26 eV and IE(*i*-PrSH) = 9.14 eV³⁸). The peaks at m/z 43 and 42 correspond to the products of unimolecular dissociation of the two isomers in the quadrupole (base peaks in the CA spectra), and the other peaks presumably arise from collision-induced dissociation even at the low kinetic energy used.

NO $^+$ is still observed for the products of decarbonylation, but it is most probably due to the contribution of the classical ions; the ratio m/z 42/ m/z 43 is now reversed and the peaks at m/z 64 and 72 (corresponding probably to H $_2$ S $^+$ transfer and C $_3$ H $_6^+$ to NO \bullet , respectively) are significantly enhanced (Figure 8f). These peaks are therefore ascribed to the distonic species.

n-Propane thiol molecular ions **4a** and the [M–CO] $^{\bullet+}$ ions of *S*-*n*-propyl thioformate **4** have been studied in the same way. Although the CA and NR spectra were found to be different from those of the isopropyl analogs, indicating different structures, the evolution of the intensities on going from the thiol to the thioformate was found identical. It is therefore clear that mixtures of classical (CH $_3$ CH $_2$ CH $_2$ SH $^+$) and distonic (CH $_3$ C \bullet HCH $_2$ S $^+$ H $_2$) ions are also formed in this case with relative proportions dependent on the origin of the ions. Note that the isomerization of 2-butane thiol ions into distonic species has recently been invoked in the literature³⁹ in order to explain the observed loss of H $_2$ S upon electron impact.

Conclusions

Using a combination of tandem mass spectrometry techniques including ion–molecule reactions, it is shown that the decarbonylation of the *S*-alkyl thioformate (R > CH $_3$) molecular ions gives rise to distonic ions besides their conventional isomers. It is tentatively proposed that sulfuranes and hydrogen-bridged species are intermediates in these decarbonylation processes. The distonic ions produced in these reactions are β -distonic ions. Their neutralization produces hypervalent diradicals expected to fragment (at least in part) spontaneously into H $_2$ S plus an olefin before reionization.

Direct ionization of alkane thiols leads also to mixtures of classical and distonic species with however an increased proportion of the classical structures. In the case of ethane thiol, MO calculations predict that the classical structure is the most stable and that the height of the isomerization energy barrier between both classical and β -distonic structures through a direct 1,3-H shift is much lower than energy thresholds for fragmentation. Theoretical results thus fully support experimental observations.

Acknowledgment. The Mons laboratory thanks the “Fonds National de la Recherche Scientifique” for its contribution in the acquisition of a large-scale tandem mass spectrometer, Micromass AutoSpec 6F. M.T.N. thanks the Fonds voor Wetenschappelijk Onderzoek (FWO-Vlaanderen) and the KULeuven (GOA) for continuing support.

References and Notes

(1) Yates, B. F.; Bouma, W. J.; Radom, L. *J. Am. Chem. Soc.* **1984**, *106*, 5805.

- (2) Hammerum, S. *Mass Spectrom. Rev.* **1988**, *7*, 123.
 (3) Stirk, K. M.; Kiminkinen, L. K. M.; Kenttämää, H. I. *Chem. Rev.* **1992**, *92*, 1649.
 (4) Golding, B. T.; Radom, L. *J. Am. Chem. Soc.* **1976**, *98*, 6331.
 (5) Bouma, W. J.; Nobes, R. H.; Radom, L. *J. Am. Chem. Soc.* **1983**, *105*, 1743.
 (6) Terlouw, J. K.; Heerma, W.; Dijkstra, G. *Org. Mass Spectrom.* **1981**, *16*, 326.
 (7) Stirk, K. G.; Kenttämää, H. I. *J. Phys. Chem.* **1992**, *96*, 5272.
 (8) Hoz, T.; Sprecher, M.; Basch, H. *J. Mol. Struct.* **1987**, *150*, 51.
 (9) Lahem, D.; Flammang, R.; Van Haverbeke, Y.; Nguyen, M. T. *Rapid Commun. Mass Spectrom.* **1997**, *11*, 373.
 (10) Lahem, D.; Flammang, R.; Nguyen, M. T. *Bull. Soc. Chim. Belg.*, in press.
 (11) Flammang, R.; Van Haverbeke, Y.; Braybrook, C.; Brown, J. *Rapid Commun. Mass Spectrom.* **1995**, *9*, 795.
 (12) (a) Bateman, R. H.; Brown, J.; Lefevre, M.; Flammang, R.; Van Haverbeke, Y. *Int. J. Mass Spectrom. Ion Processes* **1992**, *115*, 205. (b) Brown, J.; Flammang, R.; Govaert, Y.; Plisnier, M.; Wentrup, C.; Van Haverbeke, Y. *Rapid Commun. Mass Spectrom.* **1992**, *6*, 249.
 (13) Gerbaux, P.; Van Haverbeke, Y.; Flammang, R.; Wong, M. W.; Wentrup, C. *J. Phys. Chem.* **1997**, *101*, 6970.
 (14) Bax, P. C.; Holsboer, D. H.; Van der Veeck, A. P. M. *Rec. Trav. Chim.* **1971**, *90*, 562.
 (15) Frisch, M. J. L.; Trucks, G. W.; Schlegel, H. B.; Gill, P. M. W.; Johnson, B. G.; Robb, M. A.; Cheeseman, J. R.; Keith, T.; Petersson, G. A.; Montgomery, J. A.; Raghavachari, K.; Al-Laham, M. A.; Zakrzewski, V. G.; Ortiz, J. V.; Foresman, J. B.; Cioslowski, J.; Stefanov, B. B.; Nanayakkari, A.; Challacombe, M.; Peng, C. Y.; Ayala, P. Y.; Chen, W.; Wong, M. W.; Andres, J. L.; Replogle, E. S.; Gomperts, R.; Martin, R. L.; Fox, D. J.; Binkley, J. S.; Defrees, D. J.; Baker, J.; Stewart, J. P.; Head-Gordon, M.; Gonzalez, C.; Pople, J. A. *Gaussian 94*, Revision C.3; Gaussian, Inc.: Pittsburgh, PA, 1995.
 (16) Yates, B. F.; Bouma, W. J.; Radom, L. *J. Am. Chem. Soc.* **1987**, *109*, 2250.
 (17) Nguyen, M. T.; Landuyt, L.; Vanquickenborne, L. G. *Chem. Phys. Lett.* **1991**, *182*, 275.
 (18) Holmes, J. L.; Lossing, F. P.; Terlouw, J. K.; Burgers, P. C. *Can. J. Chem.* **1983**, *61*, 2305.
 (19) Beranová, S.; Wesdemiotis, C. *J. Am. Soc. Mass Spectrom.* **1994**, *5*, 1093.
 (20) (a) Wiedman, F. A.; Cai, J.; Wesdemiotis, C. *Rapid Commun. Mass Spectrom.* **1994**, *8*, 804. (b) Flammang, R.; Van Haverbeke, Y.; Wong, M. W.; Wentrup, C. *Rapid Commun. Mass Spectrom.* **1995**, *9*, 203.
 (21) Heinrich, N.; Drewello, T.; Burgers, P. C.; Morrow, J. C.; Schmidt, J.; Kulik, W.; Terlouw, J. K.; Schwarz, H. *J. Am. Chem. Soc.* **1992**, *114*, 3776.
 (22) Lahem, D.; Flammang, R.; Nguyen, M. T. *Chem. Phys. Lett.* **1997**, *270*, 83.
 (23) Weiske, T.; van der Wel, H.; Nibbering, N. M. M.; Schwarz, H. *Angew. Chem., Int. Ed. Engl.* **1984**, *23*, 733.
 (24) Gerbaux, P.; Van Haverbeke, Y.; Flammang, R. *J. Mass Spectrom.* **1997**, *32*, 1170.
 (25) Baumann, B. C.; MacLeod, J. K.; Radom, L. *J. Am. Chem. Soc.* **1980**, *102*, 7927.
 (26) Verma, S.; Ciupek, J. D.; Cooks, R. G. *Int. J. Mass Spectrom. Ion Processes* **1984**, *62*, 219.
 (27) Bouchoux, G. *Mass Spectrom. Rev.* **1988**, *7*, 1.
 (28) Kiminkinen, L. K. M.; Stirk, K. G.; Kenttämää, H. I. *J. Am. Chem. Soc.* **1992**, *114*, 2027.
 (29) Kenttämää, H. I.; Kiminkinen, L. K. M.; Orłowski, J. C.; Stirk, K. M. *Rapid Commun. Mass Spectrom.* **1992**, *6*, 734.
 (30) Vogt, J.; Williamson, A. D.; Beauchamp, J. L. *J. Am. Chem. Soc.* **1978**, *100*, 3478.
 (31) Armitage, M. A.; Higgins, M. J.; Lewars, E. G.; March, R. E. *J. Am. Chem. Soc.* **1980**, *102*, 5064.
 (32) Iraqi, M.; Lifshitz, C.; Reuben, B. G. *J. Phys. Chem.* **1991**, *95*, 7742.
 (33) Wentrup, C.; Gross, G.; Berstermann, H.-M.; Lorencak, P. *J. Org. Chem.* **1985**, *50*, 2877.
 (34) Maquestiau, A.; Pauwels, P.; Flammang, R.; Lorencak, P.; Wentrup, C. *Org. Mass Spectrom.* **1986**, *21*, 259.
 (35) Postma, R.; van Helden, S. P.; van Lenthe, J. H.; Ruttink, P. J. A.; Terlouw, J. K.; Holmes, J. L. *Org. Mass Spectrom.* **1988**, *23*, 503.
 (36) Holmes, J. L.; Osborne, A. D. *Int. J. Mass Spectrom. Ion Phys.* **1977**, *23*, 189.
 (37) The parent H $_3$ S \bullet radical has recently been shown to exist as a metastable species: Sadilek, M.; Turecek, F. *J. Phys. Chem.* **1996**, *100*, 15027. See also Nguyen, V. Q.; Sadilek, M.; Ferrier, J.; Frank, A. J.; Turecek, F. *J. Phys. Chem.* **1997**, *101*, 3789.
 (38) Lias, S. G.; Bartmess, J. E.; Liebman, J. F.; Holmes, J. L.; Levin, R. D.; Mallard, W. G. *J. Phys. Chem. Ref. Data* **1988**, *17*, Suppl. 1.
 (39) Soh, E.; Mayer, P. M.; Baer, T. *Int. J. Mass Spectrom. Ion Processes* **1997**, *160*, 63.